Copy No. _____

Defence Research and Development Canada
Recherche et développement pour la défense Canada

DEFENCE R&D DÉFENSE

Calculations of reverberation and fathometer returns at short times using a straight-line ray-path model

Dale D. Ellis

Defence R&D Canada – Atlantic

Technical Memorandum
DRDC Atlantic TM 2011-323
February 2012

Canada

This page intentionally left blank.

Calculations of reverberation and fathometer returns at short times using a straight-line ray-path model

Dale D. Ellis

Defence R&D Canada – Atlantic
Technical Memorandum
DRDC Atlantic TM 2011-323
February 2012

Principal Author

Original signed by Dale D. Ellis

Dale D. Ellis

Approved by

Original signed by Dan Hutt

Dan Hutt
Head/Underwater Sensing Section

Approved for release by

Original signed by Calvin Hyatt

Calvin Hyatt
Chair/Document Review Panel

Abstract

A straight-line ray-path model has been developed to calculate reverberation and fathometer returns at short times. Previous calculations of reverberation at long ranges/times have shown good agreement among various models, with very little dependence on the receiver depth. However, at times less than a few seconds the steep-angle scattering and fathometer returns begin to dominate, so normal mode and other waveguide models begin to break down, but ray models are quite efficient. At very short times the fathometer returns completely dominate, and there is a strong dependence on the receiver depth. The reverberation is calculated assuming the scattered energy in the various multipath arrivals is summed incoherently. However, the fathometer returns are specular reflections and the pressure from each arrival should be summed coherently. The equations for the model are presented, and illustrated by a number of examples from Problem XI of the Reverberation Modeling Workshop. This problem has a vertically bistatic source-receiver geometry in 100 m of isovelocity water over a flat sand-like bottom with Lambert scattering. The pulse is a Gaussian-shaded CW, with a bandwidth of 1/20 of the centre frequency. In this model the calculations show that at higher frequencies (e.g., 3500 Hz) the individual fathometer returns can be clearly seen, but at lower frequencies (e.g., 250 Hz) the pulse is longer and the returns overlap. In this case the method of fathometer summation selected, coherent or incoherent, is significant as well as the details of the pulse shape. Particularly interesting is the receiver at the source depth (monostatic case) where a pair of fathometer returns have identical amplitudes and phases so add coherently, compared with a receiver just a half-wavelength apart, where the fathometers essentially cancel.

Résumé

On a conçu un modèle de trajet d'ondes linéaire visant à calculer les échos de réverbération et de sondeurs à ultrasons en présence de courts délais. Des calculs antérieurs de réverbération à longue portée et à long délai ont révélé une bonne concordance entre les divers modèles et une très faible dépendance quant à la profondeur du récepteur. Toutefois, lorsque les délais n'étaient que de quelques secondes, les échos de diffusion à angle prononcé et de sondeur à ultrasons commençaient à dominer, de sorte que l'efficacité des modèles de guide d'ondes (notamment en mode normal) commençaient à diminuer, tandis que celle des modèles de trajet demeurait très grande. Dans le cas de délais très courts, les échos de sondeur à ultrasons dominaient complètement, et la profondeur du récepteur influait fortement. On calcule la réverbération en tenant pour acquis que l'énergie diffusée dans les diverses arrivées multitrajets est calculée de façon incohérente. Or, les échos de sondeur à ultrasons sont des réflexions spéculaires qui exigent une addition cohérente de la pression à chaque arrivée. Le rapport comporte les équations du modèle, qu'on illustre au moyen d'un certain nombre d'exemples tirés du problème XI des ateliers de modélisation de réverbération. Ce problème présente une géométrie de récepteur-source verticalement bistatique sous 100 m d'eau isovèle, au-dessus d'un fond plat de type sablonneux et en présence d'une diffusion de Lambert. L'impulsion est composée d'ondes CW à décroissance gaussienne dont la largeur de bande correspond à 1/20 de la fréquence centrale. Les calculs du modèle montrent qu'en présence de fréquences supérieures (p. ex. 3500 Hz) on peut clairement observer chaque écho des sondeur à ultrasons, mais qu'en présence de fréquences inférieures (p. ex. 250 Hz), on obtient une impulsion plus longue et un chevauchement d'échos. Dans ce dernier cas, le choix de la méthode d'addition (cohérente ou incohérente) des échos de sondeur à ultrasons et les caractéristiques de la forme de l'impulsion jouent un rôle important. Il est particulièrement intéressant de noter que dans le cas d'un récepteur situé à la même profondeur qu'une source (cas monostatique), les amplitudes et les phases d'une paire d'échos de sondeur à ultrasons sont identiques (et s'additionnent donc de façon cohérente), alors que dans le cas d'un récepteur situé à une demi-longueur d'onde de la source, ces échos s'annulent essentiellement.

Executive summary

Calculations of reverberation and fathometer returns at short times using a straight-line ray-path model

Dale D. Ellis; DRDC Atlantic TM 2011-323; Defence R&D Canada – Atlantic; February 2012.

Background: The 2006 and 2008 Reverberation Modeling Workshops (RMWs) described a number of test problems for various shallow water scenarios. Good agreement between the various reverberation models was achieved at long times, but discrepancies appeared at short times, where the steep-angle scattering and fathometer returns begin to dominate. The author had exercised his normal mode reverberation model on a number of the problems, but it was not suitable for extension to short times. However, ray models are well suited to handle the steep angles and short time effects. In 1987 the author had developed a simple straight-line ray trace for deep water, where the source and receiver were close to the surface. For this work the formulation was generalized to handle coherent sources and the shallow water scenarios. Also, the author had developed a straight-line ray-trace pulse propagation code `Becky` in 2004 for another project, so much of the computational framework was already in place.

Results: This paper describes the short range reverberation model `Becky_rvb` which calculates the short range reverberation and fathometer returns. The reverberation is calculated assuming the scattered energy in the various multipath arrivals is summed incoherently. However, the fathometer returns are specular reflections and the pressure from each arrival should be summed coherently. The equations for the model are presented, and illustrated by a number of examples from Problem XI of the Reverberation Modeling Workshop. The basic environment is a Pekeris waveguide, over a sand-like bottom with Lambert bottom scattering.

The pulse is a Gaussian-shaded CW, with a bandwidth of 1/20 of the centre frequency. At the ONR workshops there was considerable confusion about the definition of the pulse, so a discussion of it is included here.

Previous calculations of reverberation at long ranges/times have shown good agreement among various models, with very little depth dependence on the receiver. However, at times less than a few seconds the steep-angle scattering and fathometer returns begin to dominate. At very short times the fathometer returns completely dominate, and there is a strong dependence on the receiver depth. The calculations show that at higher frequencies (e.g., 3500 Hz) the individual fathometer returns can

be clearly seen, but at lower frequencies (e.g., 250 Hz) the pulse is longer and the returns overlap. In this case the method of fathometer summation selected, coherent or incoherent, is significant as well as the details of the pulse shape. Particularly interesting is the receiver at the source depth (monostatic case) where a pair of fathometer returns have identical amplitudes and phases so add coherently, compared with a receiver just a half-wavelength apart, where the fathometers essentially cancel.

Significance: Most sonar models treat both the reverberation and the fathometer returns incoherently. In reality the reverberation is predominantly incoherent, but the fathometer returns are specular reflections. The analysis here shows that when these arrivals overlap in time they need to be treated coherently.

The very short times and ranges for this shallow water scenario may seem academic, but when scaled to deep water, say 3000 m depth, where the first fathometers arrive near 4 s, looking for a target amid the fathometers and steep angle reverberation is quite a relevant problem.

The straight-line ray-path model provides a fast, intuitive, and simple "benchmark" for more accurate wave models. Some of the results presented here are to be included in a journal manuscript of which the PI is a co-author.

Future Work: No additional future work is planned, except to include these results as part of the journal paper.

It would be relatively straightforward to extend the predictions to other problems from the Reverberation Modeling Workshop (i.e., other scattering functions in isovelocity water), and to incorporate an approximate correction for the sound speed gradient to handle short range effects for additional problems. It would also be useful to extend the model to handle target echo, both coherently and incoherently.

Sommaire

Calculations of reverberation and fathometer returns at short times using a straight-line ray-path model

Dale D. Ellis ; DRDC Atlantic TM 2011-323 ; R & D pour la défense Canada – Atlantique ; février 2012.

Contexte : Durant les ateliers sur la modélisation de réverbération tenus en 2006 et en 2008, on a décrit un certain nombre de problèmes d'essai liés à divers scénarios en eau peu profonde. Dans le cas de longs délais, les divers modèles de réverbération concordaient bien, mais des incohérences survenaient en présence de courts délais, situation dans laquelle la présence d'échos de sondeur à ultrasons et de diffusion à angle prononcé devenait plus imposante. L'auteur a appliqué son modèle de réverbération en mode normal pour traiter un certain nombre de problèmes, mais celui-ci ne convenait pas aux courts délais, contrairement aux modèles de trajet d'ondes qui, quant à eux, s'adaptent bien aux effets des angles prononcés et des courts délais. En 1987, l'auteur a conçu un tracé de trajet linéaire destiné aux eaux profondes, selon lequel la source et le récepteur se trouvaient près de la surface. La formule a été généralisée pour ces travaux, afin de prendre en charge des sources cohérentes et des scénarios en eau peu profonde. L'auteur a également élaboré `Becky` en 2004, soit un code de propagation pulsée à tracé d'ondes linéaire destiné à un autre projet, de sorte qu'une grande partie du cadre de calcul était donc déjà en place.

Résultats : Le présent rapport porte sur le modèle de réverbération à courte portée `Becky_rvb`, qui calcule les échos à courte portée de réverbération et de sondeur à ultrasons. On calcule la réverbération en tenant pour acquis que l'énergie diffusée dans les diverses arrivées multitrajets est additionnée de façon incohérente, alors que les échos de sondeur à ultrasons sont des réflexions spéculaires qui exigent une addition cohérente de la pression à chaque arrivée. Le rapport comporte les équations du modèle, qu'on illustre au moyen d'un certain nombre d'exemples tirés du problème XI de l'atelier de modélisation de réverbération. Le milieu de base est un guide d'ondes Pekeris, au-dessus d'un fond de type sablonneux et en présence d'une diffusion de fond de Lambert.

L'impulsion est composée d'ondes CW à décroissance gaussienne dont la largeur de bande correspond à 1/20 de la fréquence centrale. Le présent rapport comporte une discussion sur la définition de cette impulsion, car celle-ci a provoqué beaucoup de confusion lors des ateliers de l'ONR.

Des calculs antérieurs de réverbération à longue portée et à long délai ont montré une bonne concordance entre les divers modèles et une très faible dépendance quant à la

profondeur du récepteur. Toutefois, lorsque les délais n'étaient que de quelques secondes, les échos de diffusion à angle prononcé et de sondeur à ultrasons commençaient à dominer. Dans le cas d'un délai très court, les échos de sondeur à ultrasons dominaient complètement, et la profondeur du récepteur influaient fortement. Les calculs ont montré qu'en présence de fréquences supérieures (p. ex. 3 500 Hz), on peut clairement observer chaque échos de sondeur à ultrasons, mais qu'en présence de fréquences inférieures (p. ex. 250 Hz), on obtient une impulsion plus longue et un chevauchement d'échos. Dans ce dernier cas, la méthode d'addition (cohérente ou incohérente) des échos de sondeurs à ultrasons et les caractéristiques de la forme d'une impulsion jouent un rôle important. Il est particulièrement intéressant de noter que dans le cas d'un récepteur situé à la même profondeur qu'une source (cas monostatique), les amplitudes et les phases d'une paire d'échos de sondeurs à ultrasons sont identiques (et s'additionnent donc de façon cohérente), alors que dans le cas d'un récepteur situé à une demi-longueur d'onde de la source, ces échos s'annulent essentiellement.

Portée : La plupart des modèles de sonar traitent les échos de réverbération et de sondeur à ultrasons de façon incohérente. En réalité, la réverbération est principalement incohérente, mais les échos de sondeur à ultrasons sont des réflexions spéculaires. L'analyse contenue dans le rapport montre que si les échos se chevauchent dans le temps, ils doivent être traités de façon cohérente.

Bien que les délais très courts et les portées très courtes du scénario en eau peu profonde puissent sembler spéculatifs, si on applique ceux-ci à un scénario en eau profonde, par exemple en présence de premiers échos de sondeur à ultrasons survenant à un délai de près de 4 s et à une profondeur de 3 000 m, chercher un objectif parmi les échos de sondeurs et de réverbération à angle prononcé pose un problème très pertinent.

Le modèle à trajet d'ondes linéaire se veut une « référence » rapide, intuitive et simple, afin d'obtenir des modèles d'ondes plus exacts. Certains des résultats présentés dans le rapport feront l'objet d'un article, dont le chercheur principal est coauteur.

Recherches futures : Outre l'ajout des résultats obtenus à l'article susmentionné, on ne prévoit pas davantage de travaux.

Il serait plutôt simple d'appliquer les prévisions obtenues à d'autres problèmes issus de l'atelier de modélisation de réverbération (d'autres fonctions de diffusion en eau isovèle) et d'incorporer une correction approximative au gradient de vitesse du son, afin de prendre en charge les effets d'une portée courte pour des problèmes supplémentaires. Il serait également utile de modifier le modèle de manière à ce qu'il prenne en charge les échos d'objectifs de façon cohérente et incohérente.

Table of contents

List of figures

Acknowledgements

This work was stimulated by the 2006 and 2008 Reverberation Modeling Workshops organized through the US Office of Naval Research and SPAWAR. Additional refinements were done for the Workshop on Validation of Sonar Performance Assessment Tools, held at Cambridge, UK in 2010. Discussions with the participants at the Workshops were very useful. Particularly valuable were discussions with Michael Ainslie of TNO in the Netherlands.

A portion of this work was conducted at the Applied Research Laboratory of The Pennsylvania State University, where the author was supported by ONR Code 32.

1 Introduction

The ONR Reverberation Modeling Workshops (RMWs) Perkins and Thorsos (2007), Thorsos and Perkins (2008), Perkins and Thorsos (2009) and Cambridge Workshop on Validation of Sonar Performance Tools Ainslie (2010b,a) described a number of test cases for various shallow water scenarios. Good agreement between the various reverberation models was achieved at long times, but discrepancies appeared at short times. At times less than a few seconds the steep-angle scattering and fathometer returns begin to dominate, so normal mode and other waveguide models begin to break down. The author had exercised his normal mode reverberation model Ellis (1995) on a number of the problems Ellis (2008), but it was not suitable for extension to short times.

However, ray models are well suited to handle the steep angles and time effects, and the author had previously developed a simple straight-line ray trace for deep water Ellis and Franklin (1987), where the source and receiver were close to the surface. In fact, the 4 bottom-bounce paths were assumed to be identical, but were added incoherently. The fathometer returns were also added incoherently, since the sources were explosives and the paths assumed not to overlap or add coherently.

For the RMW shallow-water scenarios it was necessary to generalize the deep water model, since the source and receivers were not near the surface. As well, the multiple boundary reflections from the low frequency pulse overlap, so they should be combined coherently. The author had recently developed a straight-line ray-trace pulse propagation code `Becky` for another project, so much of the computational framework was already in place.

This paper describes the short range reverberation model `Becky_rvb` which calculates the short range reverberation and fathometer returns. The reverberation is calculated incoherently, and the fathometer returns can be calculated coherently or incoherently. The basic environment is the Reverberation Modeling Workshop Problem XI, which is to calculate the reverberation in a Pekeris waveguide, over a sand-like bottom with Lambert bottom scattering.

The equations are first presented, then a description of the pulse, followed by a number of calculations, and discussion of the results.

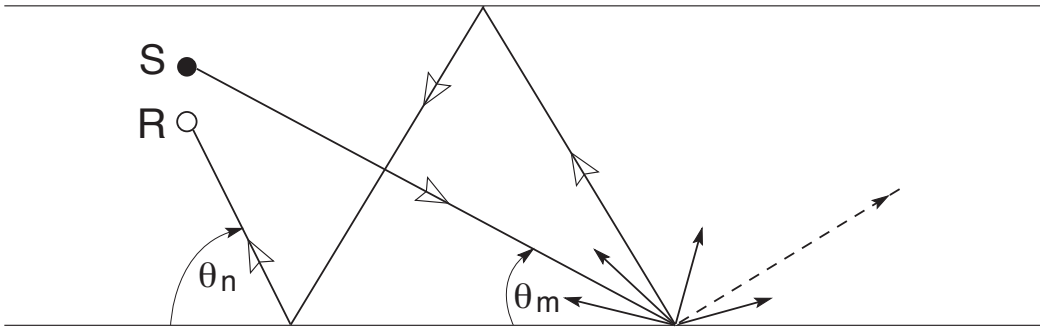

Figure 1: *Schematic of bottom reverberation in the single scatter approximation.*

2 Mathematical formulation

2.1 Reverberation expression

Figure 1 illustrates a ray picture of bottom reverberation. Energy along one path m from the source hits the bottom at some grazing angle θ_m. Most of it is reflected and continues in the specular direction (dotted line), but there is scattering into all angles; one path n back to the receiver at grazing angle θ_n is shown. The reverberation is the sum of the contributions from all the outgoing and returning contributions. In the single scattering approximation, there is only one scattering for each (m, n) pair; the other bottom or surface interactions are assumed to be specular, though reflection losses can occur.

In a uniform environment the reverberation as a function of time from a boundary can be written as

$$R(t) = \iint_{A(t)} \sum_M \sum_N I_0(t - t_{MN}) L_M(r) L_M^{'}(r) S_b(\theta_M, \theta_N)\, dA, \tag{1}$$

where $L_M(r)$ is the propagation factor (or loss) for path M from the source to the scattering patch at range r, $L_N^{'}(r)$ is the propagation factor for path N from the scattering patch to the receiver, and S_b is the boundary scattering coefficient as a function of the incident angle θ_M and the scattering angle θ_N. The sums are over all the paths connecting the scattering patch to the source or receiver, t_{MN} is the round-trip travel time for path MN, and the integral is over all areas insonified by the pulse. The source pulse has pressure $p_0(\tau)$ for duration τ_0, and $I_0(\tau)$ is the mean squared pressure (see Annex A) of $p_0(\tau)$; details of the pulse are presented in Section 3.

If we assume a constant sound speed c_w in the water, then the ray paths are straight lines. It is convenient to label the paths by the number of bottom interactions m and n. For source and receiver at $r = 0$ and at depths z_s and z_r respectively, the path

lengths l to the bottom at range r are determined by

$$[l_{mi}(r)]^2 = r^2 + h_{mi}^2 \quad \text{and} \quad [l_{nj}(r)]^2 = r^2 + h_{nj}^2, \tag{2}$$

with

$$h_{mi} = (2m-1)H \mp z_s \quad \text{and} \quad h_{nj} = (2n-1)H \mp z_r, \tag{3}$$

where H is the water depth, and i and j refer to the downgoing (0) or upgoing (1) path from the source or receiver. Assuming spherical spreading, the propagation factor along each outgoing path is then

$$L_{mi} = \frac{[V_b(\theta_{mi})]^{m-1}[V_s(\theta_{mi})]^{m-1+i}}{l_{mi}} e^{-\beta_w l_{mi}}, \tag{4}$$

where $V_s(\theta)$ and $V_b(\theta)$ are the surface and bottom reflection coefficients, $\cos(\theta_{mi}) = r/l_{mi}(r)$, and β_w is the volume absorption coefficient in the water in nepers/m. Similar expressions hold for the incoming paths L_{nj}. Note that reflection includes any phase, but not any beam displacement. A common assumption for the air-water interface is a pressure release surface for which $V_s(\theta) = -1$ for all angles.

For a given path pair, the total round trip travel time is

$$t = c_w^{-1}[l_{mi}(r) + l_{nj}(r)]. \tag{5}$$

The scattering annulus has an area $|dA| = 2\pi r\, dr$, where for a pulse of length dt,

$$dr = \frac{c_w dt}{\cos\theta_{mi} + \cos\theta_{nj}} = \frac{c_w l_{mi}(r) l_{nj}(r)}{r[l_{mi}(r) + l_{nj} r)]} dt. \tag{6}$$

The area then becomes

$$|dA| = \frac{2\pi}{t} l_{mi}(r) l_{nj}(r)\, dt. \tag{7}$$

Note, however, that the reverberation variable is time, not range, so for the various paths at fixed time we have to solve for l_{mi} and l_{nj} in terms of t at the different ranges. After lots of algebra, one gets the expression for the range $r_{mi,nj}$ at time t

$$r_{mi,nj}^2 = [(c_w t)^4 - 2(c_w t)^2(h_{mi}^2 + h_{nj}^2) + (h_{mi}^2 - h_{nj}^2)^2]/(2c_w t)^2. \tag{8}$$

The reverberation due to a unit impulse ($E_0 = I_0\tau_0 = 1$) can be written as

$$R_I(t) = \frac{2\pi}{t} \sum_{m=1}^{N_{max}+1} \sum_{n=1}^{N_{max}+1-m} \sum_{i=0}^{1} \sum_{j=0}^{1} |L_{mi}|^2 |L_{nj}|^2 S_b(\theta_{mi}, \theta_{nj}) l_{mi} l_{nj}. \tag{9}$$

Note that we have arbitrarily limited the number of bottom reflections to N_{max}. Also, the M and N in Eq. (1) include the i and j summations of Eq. (9). For a pulse $I_0(\tau)$ of finite duration $[0, \tau_0]$, the reverberation can be expressed as a convolution

$$R(t) = \int_0^{\tau_0} I_0(\tau) R_I(t-\tau)\, d\tau. \tag{10}$$

2.2 Fathometer returns

The fathometer returns (or multiple vertical bottom bounce paths between the source and receiver) are specular reflections rather than scattering, so they should be combined coherently. The direct source-receiver path and source-surface-receiver path need to be included since they can interfere with the first bottom bounce path.

Using $s_{Ni} = 2NH + \chi_i$ for the N-th bottom bounce, with $\chi_1 = -z_s - z_r, \chi_2 = -z_s + z_r, \chi_3 = z_s - z_r$, and $\chi_4 = z_s + z_r$, the pressure time series at the receiver is

$$p(t) = \sum_{N=0}^{Nmax} \sum_{i=1}^{4} \frac{p_0(t - s_{Ni}/c_w)}{s_{Ni}} V_b^N(\pi/2) V_s^{N_{Si}}(\pi/2), \tag{11}$$

where the number of surface bounces $N_{Si} = N - 1, N, N, N + 1$ for $i = 1, ..., 4$, and N_{max} is the maximum number of bottom bounces to be considered. (In 100 m water 7 bottom bounces corresponds to about 1 s). For the direct and surface bounce ($N = 0$) there are only two terms in the i-summation; i.e.,

$$\frac{p_0(t - s_{03}/c_w)}{s_{03}} - \frac{p_0(t - s_{04}/c_w)}{s_{04}}, \tag{12}$$

with $s_{03} = |z_s - z_r|$ and $s_{04} = z_s + z_r$.

Volume attenuation in the water can be included by replacing each $1/s_{Ni}$ term by $\exp(-\beta_w s_{Ni})/s_{Ni}$, where β_w is in nepers/m. In practice, our pulses are short, so the final intensity time series is simply multiplied by $\exp[-2\beta_w c_w t]$ outside the summation.

The mean squared pressure $F(t)$ of $|p(t)|^2$ is then calculated and added to the reverberation to give the total received signal

$$R_T(t) = F(t) + R(t). \tag{13}$$

See Annex A for details on the calculation of $F(t)$.

For comparison with other models the fathometer returns can also be added incoherently by combining the energy each arrival with the envelope of the pulse.

$$F_I(t) = \sum_{N=0}^{Nmax} \sum_{i=1}^{4} \frac{I_0(t - s_{Ni}/c_w)}{s_{Ni}^2} |V_b(\pi/2)|^{2N} |V_s(\pi/2)|^{2N_{Si}} e^{-2\beta_w c_w t}. \tag{14}$$

3 Pulse description

A great deal of confusion surrounded the pulse definition for the ONR Workshops. To help clarify the issue, a short note [D. D. Ellis, "That Doggone Pulse," 25 June 2009]

was circulated to a number of interested people, and made available for posting to the Workshop FTP site. The material is repeated here. Subsequently, a description of the Gaussian-shaded pulse was provided for the Cambridge Workshop on Validation of Sonar Performance Tools Ainslie (2010b), and included in the problem definitions Zampolli et al. (2010a,b).

3.1 Gaussian Shaded Pulse

The source pressure time series is given by

$$p_0(t) = A_G \cos(\omega_0 t) \exp\left(-\frac{1}{2}\left(t\Delta\omega\right)^2\right), \tag{15}$$

where $\omega_0 = 2\pi f_0$, f_0 is the centre frequency, and

$$\Delta\omega = \pi B_{3dB}/\sqrt{\ln 2},$$

where B_{3dB} is the total bandwidth to the -3 dB points, and $A_G = 1\,\mu$Pa m for the RMW problems. Since this pulse is of infinite duration, some truncation will have to occur in any practical calculation. Sonar models commonly use a uniform weighting or a Hann (cosine squared) weighting for the pulse shape; we discuss the finite pulse shapes later.

The energy in the waveform is

$$E = \int_{-\infty}^{\infty} p^2(t)dt = A_G^2 \frac{\sqrt{2\pi}}{2\Delta\omega}\left(1 + \exp(-\omega_0^2/\Delta\omega^2)\right). \tag{16}$$

The second term in parenthesis is negligible in the Workshop cases, so

$$E = A_G^2 \frac{\sqrt{\ln(2)/\pi}}{2B_{3dB}} \approx 0.23486\, A_G^2/B_{3dB}. \tag{17}$$

Note that for a rectangular pulse of rms amplitude 1.0 (or peak amplitude $\sqrt{2}$) and duration $1/B_{3dB}$, the energy is $1/B_{3dB}$, which is $(1/2)\sqrt{\ln(2)/\pi}$ (i.e., 6.29192 dB) greater than the Gaussian pulse.

A pulse of unit energy is often used in reverberation calculations. The correction for $f_0/20$ bandwidths are -17.261 dB at 250 Hz, -23.282 dB at 1000 Hz, and -28.722 dB at 3500 Hz.

The pulse is also defined in the Workshop Problems in terms of the Fourier transform[1] of its spectrum $\tilde{p}(\omega)$

$$p(t) = \frac{1}{2\pi} \int_{-\infty}^{\infty} \tilde{p}(\omega) e^{-i\omega t}\, dw, \tag{18}$$

where $\omega = 2\pi f$, and for the Gaussian pulse

$$\tilde{p}(\omega) = A_G \frac{\sqrt{2\pi}}{2\Delta\omega} \left\{ \exp\left(-\frac{(\omega - \omega_0)^2}{2\Delta\omega^2} \right) + \exp\left(-\frac{(\omega + \omega_0)^2}{2\Delta\omega^2} \right) \right\}. \tag{19}$$

The frequency spectrum or energy spectrum[2] is

$$S(\omega) = \frac{1}{2} |\tilde{p}(\omega)|^2, \tag{20}$$

and satisfies the identity

$$E = \int_{-\infty}^{\infty} S(\omega) d\omega = \int_{-\infty}^{\infty} p^2(t) dt. \tag{21}$$

3.2 Realizations of the Pulse

The Gaussian shaded pulse is infinite in extent, so any practical implementations will have to use some approximation. To avoid a discontinuity, the phase of $\cos(\omega_0 t)$ should be a multiple of $\pi/2$ at the end points, so the pulse should have $N + 1/2$ cycles, where N is some integer.

A rectangular pulse of duration T_0, and amplitude A_R would have energy $A_R^2 T_0/2$. Comparing with Eq. (17), for equal energy the rectangular pulse would have amplitude

$$A_R = A_G \left(\ln(2)/\pi\right)^{1/4} / \sqrt{T_0 B_{3dB}}. \tag{22}$$

If we choose the canonical pulse length of $T_0 \approx 1/B_{3dB}$, then the denominator is approximately unity, and $A_R \approx 0.685\, A_G$.

A Hann-shaded pulse of duration T_H is given by

$$p(t) = A_H \cos(\omega_0 t) \cos^2(\pi t/T_H), \qquad -T_H/2 \le t \le T_H/2, \tag{23}$$

[1] There are various conventions for the factor of 2π in the Fourier transform and its inverse. It is not specifically mentioned in the Workshop documents, but presumably the corresponding Fourier transform of the pulse (in μPa/Hz) is $\tilde{p}(\omega) = \frac{1}{2\pi} \int_{-\infty}^{\infty} p(t) e^{i\omega t}\, dt$. In this case both transforms have the factor of $1/2\pi$, because of the integration over ω rather than f.

[2] Some earlier ONR Workshop documents had written $S(f) = 2\pi \tilde{S}(\omega) = 2\pi |\tilde{p}(\omega)|^2$.

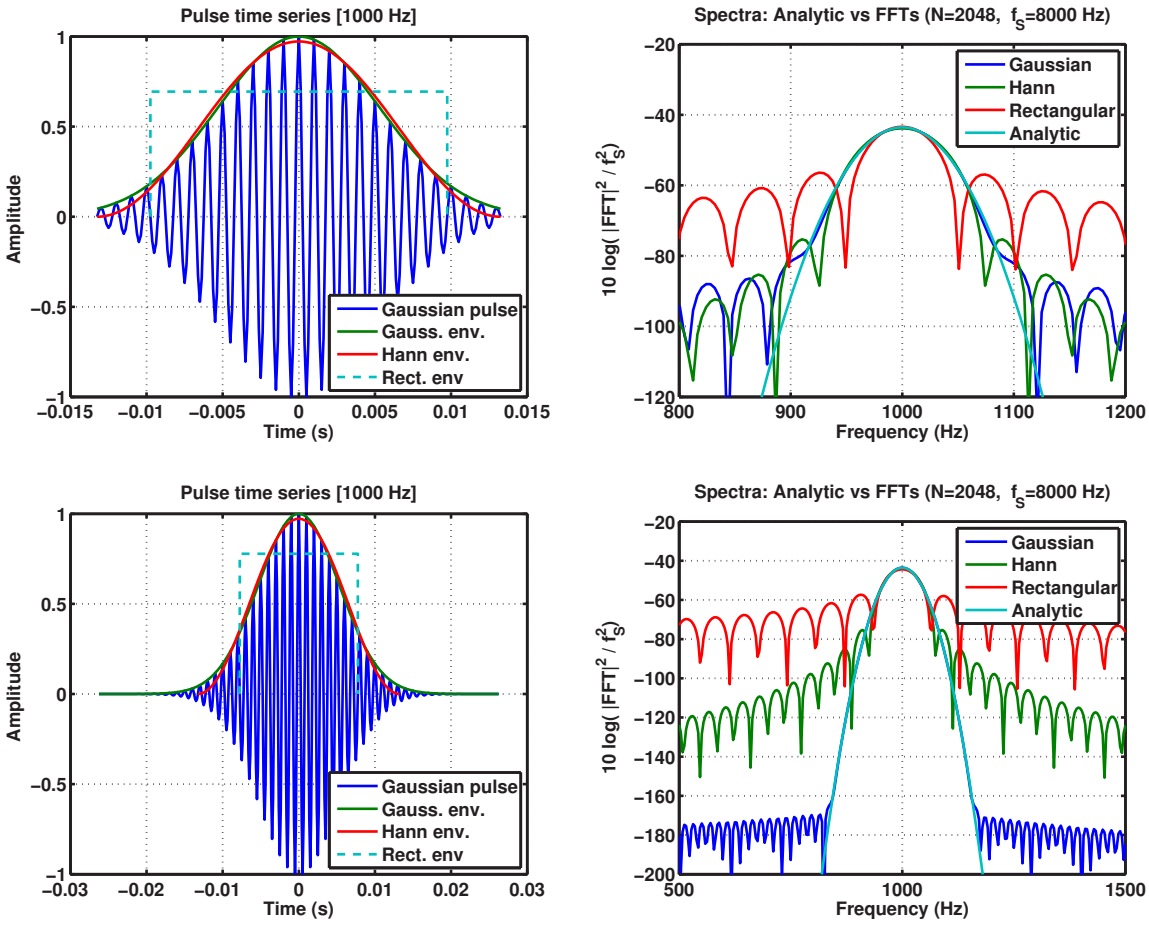

Figure 2: *Time series and spectra for several realizations of the ONR pulse at 1 kHz. The upper left figure is for a Gaussian truncated at 26.5 cycles, and the lower left for a Gaussian truncated after 52.5 cycles. The envelopes for a 26.5 cycle Hann weighted pulse are included, as well as for a uniform envelope of 19.5 cycles (upper figure) and 15.5 cycles (lower figure). The corresponding spectra are shown in the right figures.*

with energy is given by

$$E = A_H^2 \int_{-T_H/2}^{T_H/2} \cos^2(\omega_0 t) \cos^4(\pi t/T_H)\, dt \approx \frac{3}{16} A_H^2 T_H, \tag{24}$$

where $\cos^2(\omega_0 t)$ has been replaced by its average value 1/2 to approximate the integral. If T_H is an integer number of half cycles, then the r.h.s. of Eq. (24) is exact.[3] Equating Eq. (24) with the energy of the Gaussian in Eq. (17) gives

$$A_H^2 = \frac{8\sqrt{\ln(2)/\pi}}{3 T_H B_{3dB}} A_G^2. \tag{25}$$

For $T_H = 2/B_{3dB}$ (twice the duration of the canonical rectangular pulse),

$$A_H = \sqrt{4/3}\ (\ln(2)/\pi)^{1/4}\, A_G \approx 0.79 A_G. \tag{26}$$

A shorter pulse with $A_H \approx A_G$ seemed to give a better approximation to the Gaussian.

Figure 2 illustrates the time series and spectra for a number of realizations of the pulse, with $B_{3dB} = f_0/20$. The upper pair of plots illustrate the Gaussian shaded pulse truncated at 26.5 cycles, a Hann envelope of the same duration, and the envelope for a uniform weighting with 19.5 cycles (which corresponds to a duration of approximately 1/bandwidth). All pulses have the same energy in the pulse, so will produce the same average reverberation level at long ranges. The spectra on the right show that the Hann-shaded pulse reproduces the main lobe of the analytical spectrum quite closely, but the width of the main lobe for the rectangular window is too narrow. The lower plot of Fig. 2 shows the Gaussian pulse extended to 52.5 cycles. The Hann window is the same as for the upper figure, and the uniform weighting has been shortened to 15.5 cycles to better match the peak of the Gaussian spectrum. Note in the right-hand plots how extending the finite Gaussian from 26.5 cycles to 52.5 cycles has reduced the sidelobes by over 80 dB.

The details of the pulse shape are not important for the long-range reverberation, but for short times and target echo problems, the details can be significant.

[3]The exact formula for the integral (courtesy Michael Ainslie Ainslie (2007)) is

$$\begin{aligned} E &= \frac{3A_H^2 T_H}{16}\{1 + \operatorname{sinc}(\omega_0 T_H) + (1/6)[\operatorname{sinc}(2\pi + \omega_0 T_H) \\ &+ \operatorname{sinc}(2\pi - \omega_0 T_H) + 4\operatorname{sinc}(\pi + \omega_0 T_H) + 4\operatorname{sinc}(\pi - \omega_0 T_H)]\}, \end{aligned}$$

where $\operatorname{sinc}(x) = \sin(x)/x$. The correction terms are small if the product $\omega_0 T_H$ is large. Also, if ωT_H is a multiple of π, all the sinc terms become zero.

4 Calculations

We now present some calculations for RMW Problem XI, in which the environment is a Pekeris waveguide with a sand-like bottom and Lambert scattering, and the source receiver are in a vertically bistatic geometry. The reverberation as a function of time is required for a Gaussian shaded pulse at various frequencies.

The ONR Reverberation Modeling Workshop problems and various updates were first described Thorsos et al. (2006) by files on a FTP site:

`ftp://ftp.ccs.nrl.navy.mil/pub/ram/RevModWkshp`.

For the second Reverberation Modeling Workshop additional problems were proposed, with descriptions on:

`ftp://ftp.ccs.nrl.navy.mil/pub/ram/RevModWkshp_I`

`ftp://ftp.ccs.nrl.navy.mil/pub/ram/RevModWkshp_II`.

The best description is by Ainslie and co-workers for the April 2010 Workshop on Validation of Sonar Performance Assessment Tools held at Cambridge UK, and published in a conference proceedings Zampolli et al. (2010a) and as an archival article Zampolli et al. (2010b). The essential material is repeated in this paper.

4.1 Scenario Description

The environment is a Pekeris waveguide with a sand-like bottom and Lambert scattering. Specifically the water has depth 100 m, sound speed $c_w = 1500$ m/s, and density ρ_w. The upper boundary is a perfectly reflecting pressure release surface. The bottom is a halfspace with relative density $\rho_b/\rho_w = 2.0$, sound speed $c_b = 1700$ m/s, and absorption coefficient $\alpha_b = 0.5$ dB/wavelength. We use the bottom reflection loss given by the Rayleigh reflection coefficient

$$V_b(\theta) = \frac{Z_b - Z_w}{Z_b + Z_w}, \tag{27}$$

where $Z_w = \rho_w c_w / \sin\theta$ and $Z_b = \rho_b c_b' / \sin\theta_b$. The bottom grazing angle (imaginary below the critical angle) is given by Snell's law $\cos\theta_b = (c_b/c_w)\cos\theta$. Absorption in the bottom is handled by giving c_b' an imaginary component

$$c_b' = \frac{c_b}{1 + i\alpha_b(\ln 10)/(40\pi)}. \tag{28}$$

The bottom scattering is Lambert's rule

$$S_b(\theta, \theta') = \mu \sin(\theta)\sin(\theta') \tag{29}$$

with $10\log\mu = -27$, or $\mu \approx 0.002$.

A point source was at depth 30 m, and omnidirectional receivers at depths of 10, 50 and 90 m directly above or below the source. The pulse was the Gaussian shaded time series, Eq. (15), with centre frequencies f_c at 250, 1000 and 3500 Hz, and corresponding -3 dB bandwidths $f_c/20$. For the calculations it was truncated to 53 cycles.

The water column absorption in dB/km is

$$\alpha_w = 3.3 \times 10^{-3} + \frac{0.11F^2}{1+F^2} + \frac{44F^2}{4100+F^2} + 3.0 \times 10^{-4}F^2 \tag{30}$$

where $F = f_c/(1000 \text{ Hz})$. It is quite small, but at 3500 Hz is 0.24 dB/km so is not entirely negligible.

4.2 Results

4.2.1 Example of `Becky_rvb` calculations

Figure 3 shows the various components of the `Becky_rvb` model at 1 kHz for the source at 30 m and the receiver at 50 m, on both linear and logarithmic time scales. The direct arrivals and incoherently summed fathometer returns Eq. (14) are shown by the green curve; the circles show the individual terms in the summation. The direct path arrives at (20 m)/(1500 m/s) = 0.0133 s, and the surface reflected path arrives at 80/1500 = 0.053 s. The first bottom scattered path arrives at 120/1500 = 0.08 s, followed 0.04 s later by the surface-bottom arrival at 180/1500 = 0.12 s. The bottom-surface and surface-bottom-surface paths arrive at 220/1500 = 0.147 s and 280/1500 = 0.187 s. These 4 combinations repeat at 200/1500 = 0.133 s intervals. In addition to the spreading loss, the subsequent bottom bounce groups drop by the vertical incident bottom loss of 8.3 dB.

The reverberation impulse Eq. (9) is given by the red curve. It jumps upward every time a new path appears. The reverberation convolved with the pulse intensity Eq. (9) is shown in the aqua curve. The magenta curve Eq. (13) is the convolved reverberation added to the fathometers, this time calculated calculated coherently. In this case the fathometer returns are sufficiently separated in time, so it doesn't matter whether they are added coherently or incoherently. However, when the arrivals overlap there is a difference.

4.2.2 Effect of receiver depth

Figure 4 shows the various components of the `Becky_rvb` model at 10 m. The direct path arrives at 20/1500 = 0.0133 s and the surface bounce at 40/1500 = 0.0267 s. The first bottom scattered path arrives at 160/1500 = 0.107 s, followed 0.013 s later

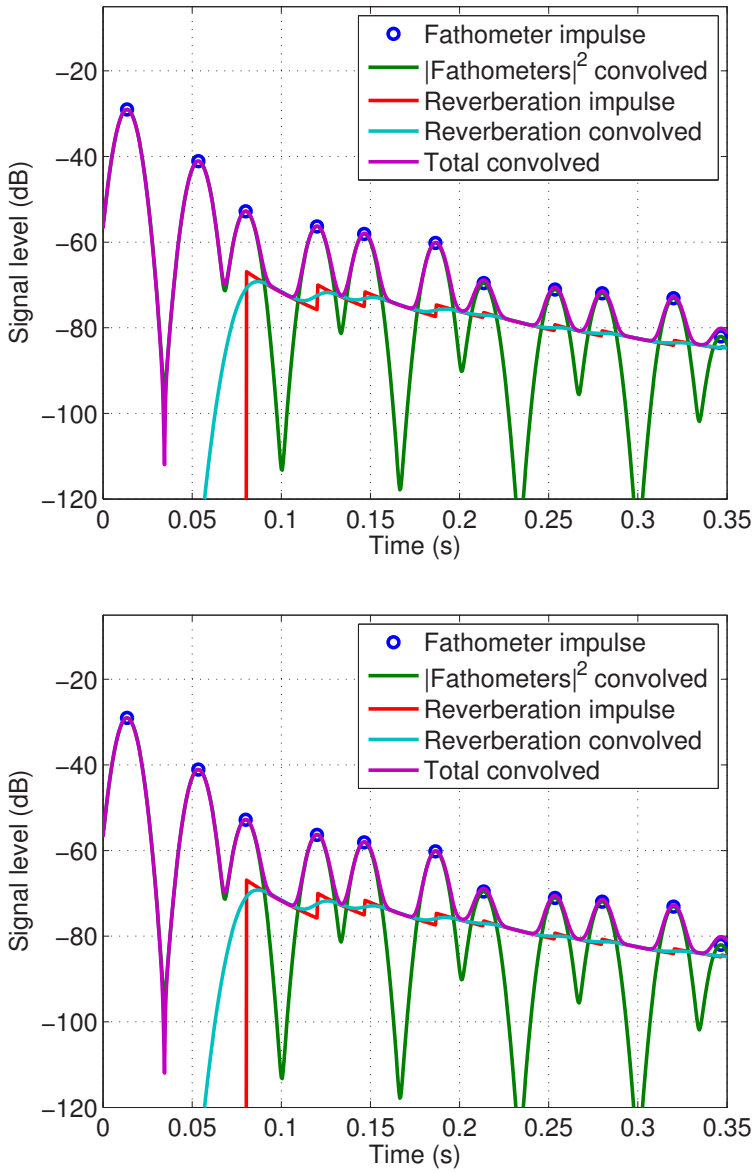

Figure 3: *Individual arrivals and impulse response at 1000 Hz for 50 m receiver; linear time axis (upper) and logarithmic time axis (lower).*

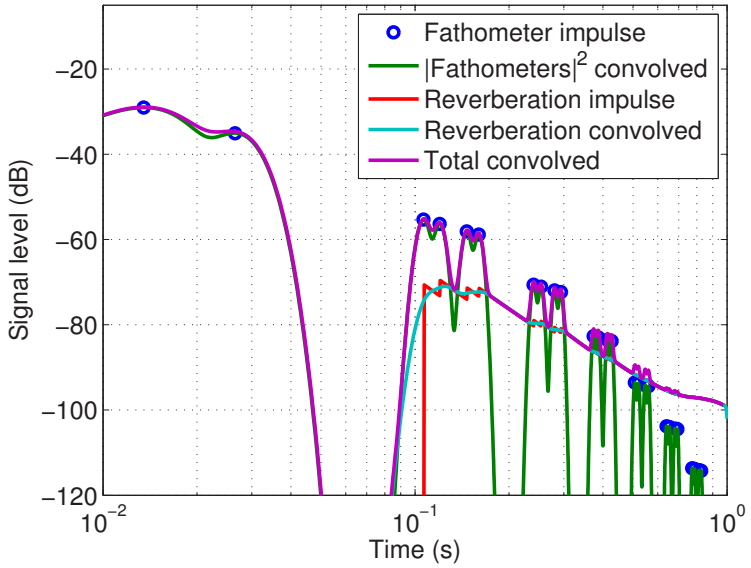

Figure 4: *Individual arrivals and impulse response at 1000 Hz for 10 m receiver.*

by the surface-bottom arrival at 180/1500 = 0.12 s. The bottom-surface and surface-bottom-surface paths arrive at 220/1500 = 0.147 s and 240/1500 = 0.160 s. These 4 combinations repeat at 200/1500 = 0.133 s intervals, reduced by the spreading loss and 8.3 dB bottom loss. There is a slight difference between the coherently and incoherently added fathometers where the 20 m separation corresponds to 13 1/3 wavelengths and the surface bounce adds another another phase change of π.

In Fig. 5 for the 90 m receiver, the direct path arrives at 0.040 s, the first bottom bounce at 20/1500 = 0.013 s later. The surface reflected path arrives at 120/1500 = 0.08 s, followed 0.013 s later by the surface-bottom arrival at 140/1500 = 0.093 s. These combinations repeat at 200/1500 = 0.133 s intervals. Our notional grouping by the number of bottom bounces is not natural for this geometry; the number of surface bounces would be more appropriate, but it does not make any difference to the results. The arrivals separated by 0.013 s (20 m separation, or 13 1/3 wavelengths) are still resolved, even with bottom loss decreasing the second arrival by 8.3 dB. This time there is no phase change from the bottom reflection, and the arrival pair tends to interfere rather than to add coherently as with the 10 m receiver. This makes sense physically: the two arrivals are only 1/6 wavelength from being out of phase, whereas with the surface receiver they are within 1/6 wavelength of being in phase.

Now consider the monostatic case where two paths have identical phase and amplitude. Figure 6 shows the various components of the `Becky_rvb` model with the receiver at 30 m. The surface reflection arrives at 0.040 s, the first bottom bounce at

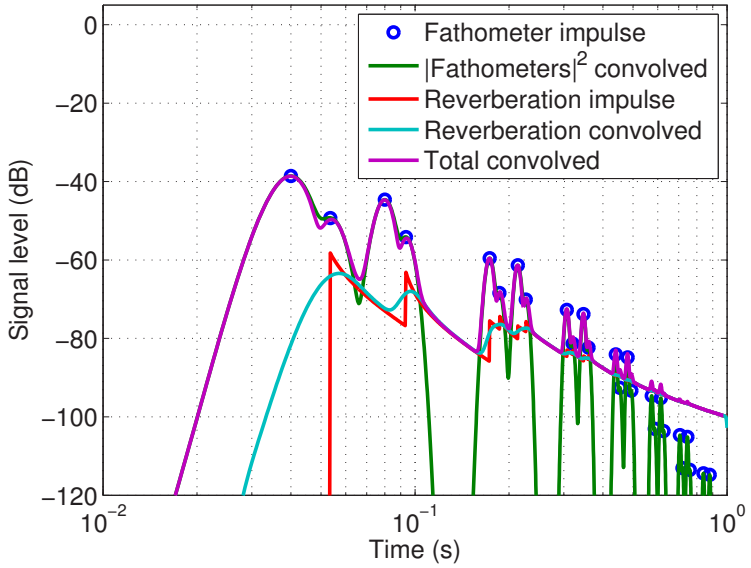

Figure 5: *Individual arrivals and impulse response at 1000 Hz for 90 m receiver.*

140/1500 = 0.093 s, the surface-bottom pair at 200/1500 = 0.133 s, and the surface-bottom-surface arrival at 260/1500 = 0.173 s. The direct path is suppressed, since the source receiver are co-located so the intensity would be infinite for the duration of the pulse. This time for the co-incident arrivals we see the 3 dB enhancement for the incoherently added fathometer returns, and a 6 dB enhancement for the coherently added fathometers.

If we shift the location of the receiver by 0.375 m, the path length of the previously-coincident pair (at about 0.133 s and other multiples) is changed by 0.75 m, or a half wavelength at 1 kHz. Figure 7 for a 30.375 m receiver at 1 kHz shows that now the coherently added fathometers (magenta curve) nearly cancel instead of adding coherently. Note that the incoherently added fathometers are essentially unchanged from the monostatic case. The reverberation is computed incoherently, so is essentially unchanged from the monostatic prediction.

4.2.3 Frequency dependence

Now we look at the frequency dependence. Figure 8 shows the results for the 50 m receiver at 3 frequencies. The direct arrival comes at 0.013 s and the surface bounce at 80/1500 = 0.053 s. The first fathometer return (and initial bottom scattering) arrive at 120/1500 = 0.080 s, and the next arrival comes 0.04 s later at 0.12 s. The time difference between arrivals is sufficient to resolve the 1.0 and 3.5 kHz pulses, but not the 250 Hz pulse.

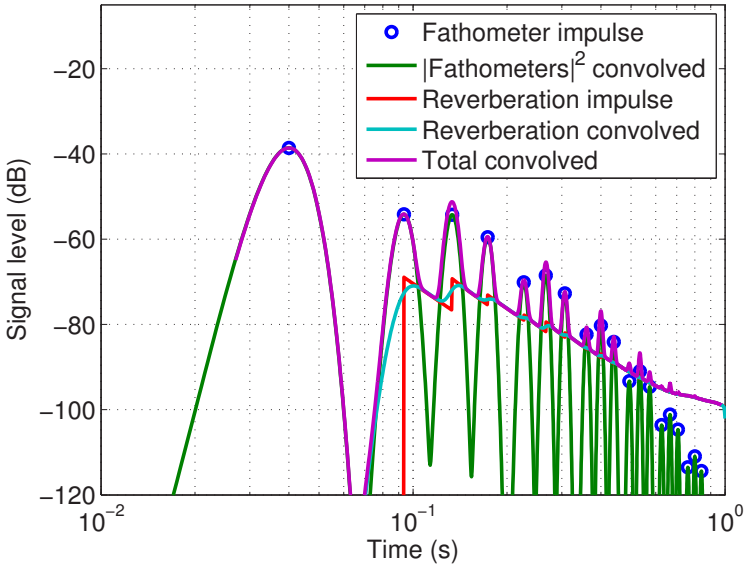

Figure 6: *Individual arrivals and impulse response at 1000 Hz for 30 m receiver.*

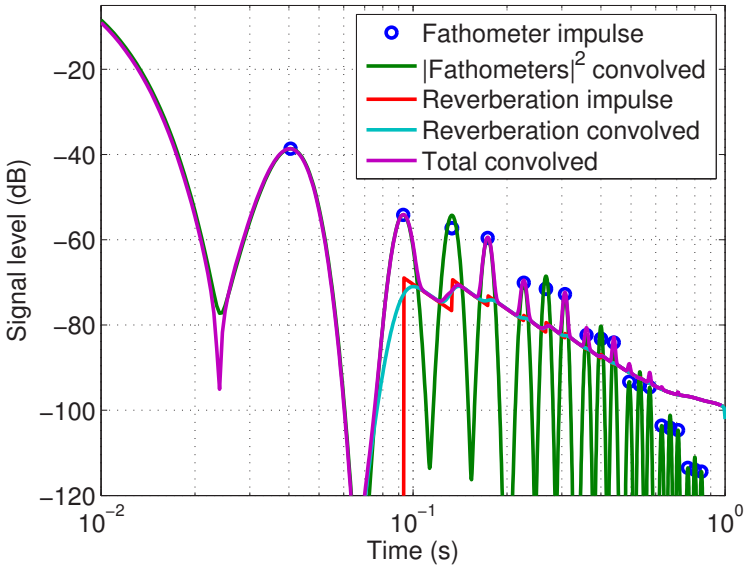

Figure 7: *Predictions of fathometer returns and short-range reverberation at 1 kHz for 30.375 m receiver.*

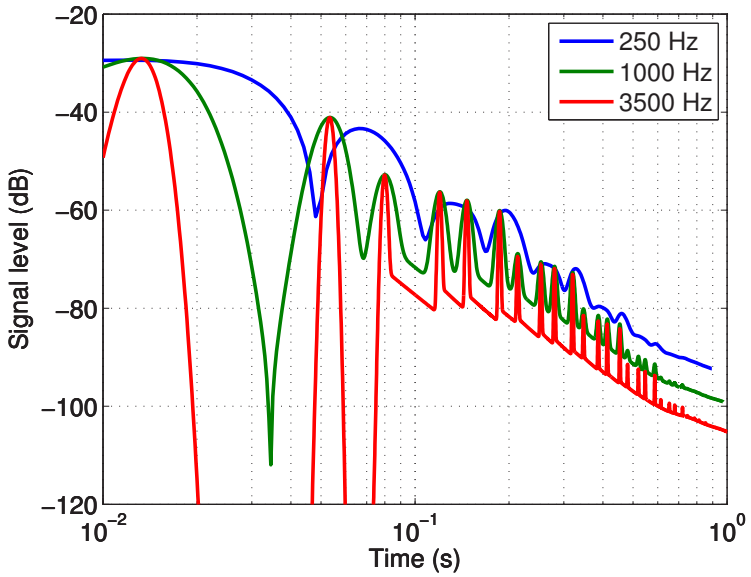

Figure 8: *Ray-trace predictions of fathometer returns and short-range reverberation for 50 m receiver.*

Figure 9 compares the predictions at 3 frequencies, but for a receiver at 10 m. The direct path arrives at $20/1500 = 0.0133$ s and the surface bounce at 0.0267 s. The various fathometer returns arrive in pairs separated by 0.0267 s. Here we see that for the 3500 Hz pulse the fathometer returns are resolved, while at 250 Hz there is considerable overlap. At 1 kHz, some pairs are barely resolved. Comparing with the plot for the 50 m receiver, it can be seen that the reverberation levels are similar, but the details of the fathometer returns are quite different. Figure 10 shows the results for the 90 m receiver at 3 frequencies.

Figure 11 shows the results for the 30 m receiver (pure monostatic geometry). In this case the receiver (being coincident with the transmitter) will be totally overloaded for the duration of the pulse.

4.2.4 Comparison with mode calculation

Figure 12 illustrates why developing the ray trace was required. It compares the NOGRP (normal mode) predictions Ellis (2008) with the predictions from `Becky_rvb` at 1 kHz, for the 30 m source and 50 m receiver. The two are in quite good agreement at 2 s (and beyond) with the ray-trace being calculations slightly higher as one would expect since there should be a small contribution from angles above the critical angle. At shorter times, the effect of the steeper angles becomes increasingly significant. The `Becky_rvb` calculations were done allowing 7 bottom bounces or 20 bottom bounces on the outgoing and return paths; 7 bottom bounces seem sufficient out to 1 s. The

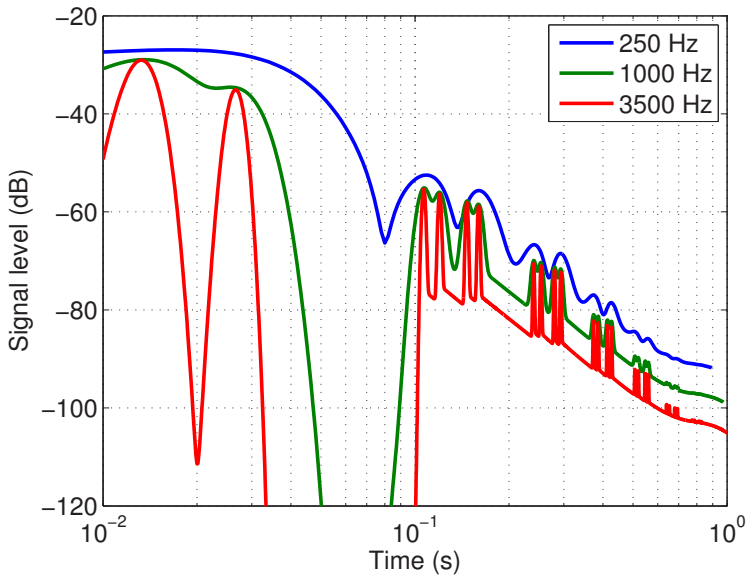

Figure 9: *Ray-trace predictions of fathometer returns and short-range reverberation for 10 m receiver.*

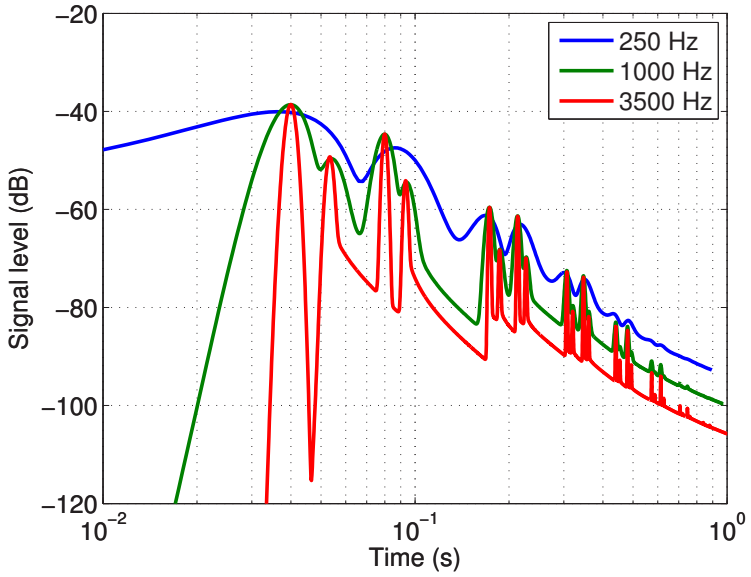

Figure 10: *Ray-trace predictions of fathometer returns and short-range reverberation for 90 m receiver.*

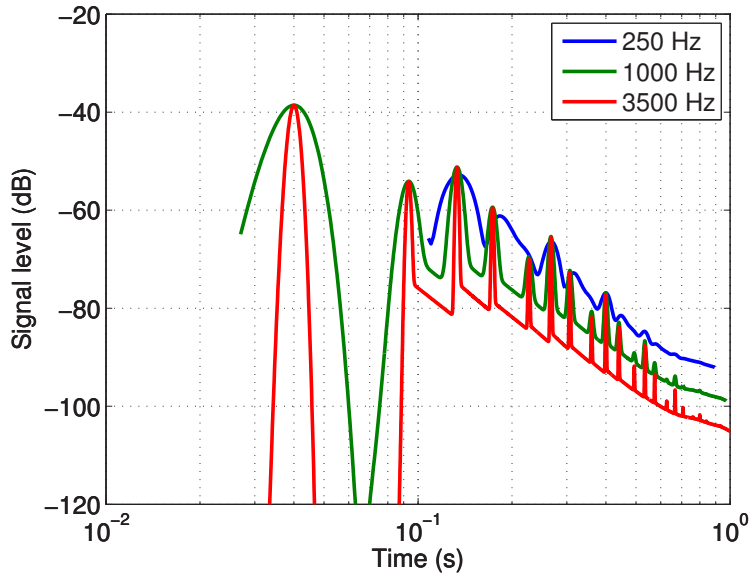

Figure 11: *Ray-trace predictions of fathometer returns and short-range reverberation for 30 m receiver (monostatic geometry).*

lower envelope of the Becky curve essentially delimits the reverberation, while the peaks are from the fathometer returns.

4.2.5 Summary of calculations

The main results can be summarized as:

- For $t > 2$ s, the ray and mode models agree
- For $t < 2$ s, the steep angle paths become increasingly important
- The main thing affecting the reverberation is the energy in the pulse
- The dominant thing affecting the fathometer returns is the peak pulse pressure
- The fathometer returns dominate at very short range
- Where the fathometer returns overlap, they should be added coherenntly
- The details of the pulse are important in determining the interference

For the 1 kHz pulse

- For $t < 0.6$ s, the fathometers start to appear above the reverberation
- For $t < 0.3$ s (or 2 bottom reflections) the fathometers completely dominate the reverberation.

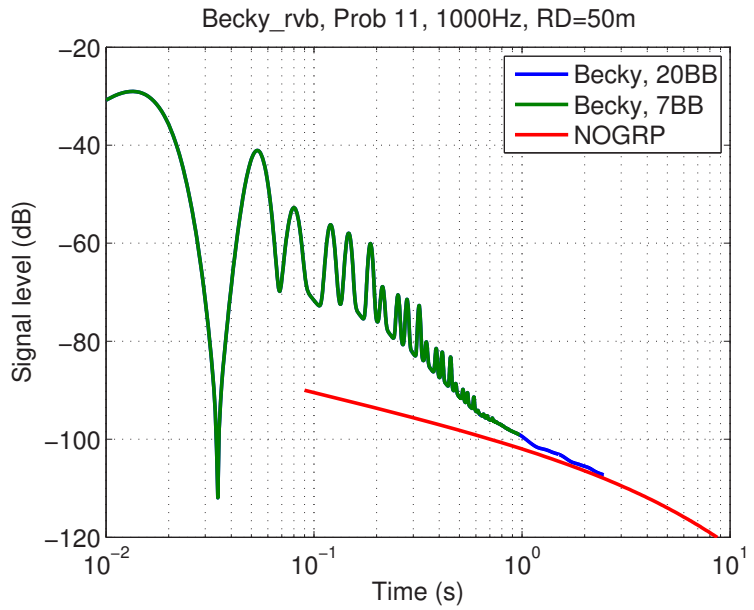

Figure 12: *Ray-trace predictions of fathometer returns and short-range reverberation compared with normal mode calculation.*

5 Discussion and concluding remarks

The ray model supplements the normal mode model at short ranges. Together they essentially form a benchmark solution to an approximation of Problem XI: single scattering, no forward scattering loss, incoherently summed reverberation.

Initial comparisons with energy flux models, analytic solutions, and normal mode models were presented at the 2007 meeting of the Acoustical Society of America Ellis et al. (2007). More detailed comparisons were subsequently done Ainslie et al. (2011) and a journal manuscript is nearing completion.

It will be interesting to compare the `Becky_rvb` model predictions with those from a full wave model with multiple realizations of a rough bottom, similar to Fromm and Lingevitch Fromm and Lingevitch (2008). Since no realizations of a Lambert bottom are readily available, the likely scenario would be RMW Problem V; the bottom scattering and boundary reflection models would have to be adapted, but the formulation would remain relevant.

Coherent effects can clearly be important for the specular reflections. For reverberation the importance of coherent effects is not so clear, though Ainslie has pointed out (private communication) that there will clearly be coherent effects for monostatic reverberation.

It may seem academic to look at times shorter than 1 s for a low frequency active sonar application. However, the Reverberation Modeling Workshop Problems did not have a deep water scenario. If one scales up to a water depth of say 3000 m, then the first fathometer return arrives at 4 s, so looking for a target echo amid the steep angle reverberation and fathometer returns is quite a relevant problem.

The model has been applied to isovelocity water. It could also be applied to other Workshop problems. For more realistic problems it can be approximately extended to water with a linear gradient as was done by Ellis and Franklin Ellis and Franklin (1987), and source receiver beam patterns can be incorporated. The approximation gives the correct angles for bottom loss and scattering, but does not correct the travel times and spreading loss. We would not expect benchmark results in this case, but it would provide a useful comparison.

In terms of relevance to sonar problems, it would be useful to apply some different pulse waveforms; e.g., rectangular or Tukey-shaded CW, Hann-shaded CW, and an LFM pulse. It would also be useful to extend the model to handle target echo, both coherently and incoherently.

References

Ainslie, M. A. (2007). TNO, Netherlands. Personal communication.

Ainslie, M. A. (2010), Editorial: Validation of Sonar Performance Assessment Tools, *Proc. Institute of Acoustics*, 32, Pt. 2, 3–6.

Ainslie, M. A. (2010), Meeting report, Validation of Sonar Performance Assessment Tools: A workshop held in memory of David E Weston, *IOA Acoustics Bulletin*, pp. 13–16.

Ainslie, M. A., Ellis, D. D., and Harrison, C. H. (2011), Towards benchmarks of low frequency reverberation level in a Pekeris waveguide: Insight from analytical solutions, *J. Acoust. Soc. Am.*, 129(5, Pt. 2 of 2), 2631. Abstract 4pUW10. Presented by M. Ainslie at 161st Meeting of the Acoustical Society of America, Seattle, WA, USA, 23–27 May 2011.

Ellis, D. D. (1995), A shallow-water normal-mode reverberation model, *J. Acoust. Soc. Am.*, 97, 2804–2814.

Ellis, D. D. (2008), Normal-mode models OGOPOGO and NOGRP applied to the 2006 ONR Reverberation Modeling Workshop problems, (Technical Memorandum TM 2006-289) DRDC Atlantic, Dartmouth, NS, Canada.

Ellis, D. D., Ainslie, M. A., and Harrison, C. H. (2007), A comparison of ray, normal-mode, and energy flux results for reverberation in a Pekeris waveguide, *J. Acoust. Soc. Am.*, 122, 3075. Abstract 4aUW9. Paper presented in special session on "Underwater Reverberation Measurements and Modeling," 154th Meeting of Acoustical Society of America, New Orleans, LA, USA, 27 Nov – 1 Dec 2007.

Ellis, D. D. and Franklin, J. B. (1987), The importance of hybrid ray paths, bottom loss, and facet reflection on ocean bottom reverberation, In Merklinger, H. M., (Ed.), *Progress in Underwater Acoustics*, pp. 75–84, International Congress on Acoustics, New York: Plenum Press.

Fromm, D. M. and Lingevitch, J. F. (2008), Semi-coherent reverberation calculations, In Nielsen et al. (Nielsen et al. 2008), pp. 47–54.

Nielsen, P. L., Harrison, C. H., and Le Gac, J.-C., (Eds.) (2008), International Symposium on Underwater Reverberation and Clutter, NATO Undersea Research Centre, La Spezia, Italy. Conference held at Villa Marigola, Lerici, Italy, 9–12 September 2008.

Perkins, J. S. and Thorsos, E. I. (2007), Overview of the reverberation modeling workshops, *J. Acoust. Soc. Am.*, 122, 3074. Abstract 4aUW1. Special session on

"Underwater Reverberation Measurements and Modeling," 154th Meeting of Acoustical Society of America, New Orleans, LA, USA, 27 Nov – 1 Dec 2007.

Perkins, J. S. and Thorsos, E. I. (2009), Update on the reverberation modeling workshops, *J. Acoust. Soc. Am.*, 126(4, Pt. 2), 2208. Abstract 2aUW1. Special session on "Reverberation Measurements and Modeling," 158th Meeting of Acoustical Society of America, San Antonio, TX, USA, 26–30 October 2009.

Thorsos, E., Perkins, J., and LePage, K. (2006), Reverberation Modeling Workshop Problem Descriptions. FTP site, ftp://ftp.ccs.nrl.navy.mil/pub/ram/RevModWkshp_I.

Thorsos, E. I. and Perkins, J. S. (2008), Overview of the reverberation modeling workshops, In Nielsen et al. (Nielsen et al. 2008), pp. 3–14. Conference held at Villa Marigola, Lerici, Italy, 9–12 September 2008.

Zampolli, M., Ainslie, M. A., and Schippers, P. (2010), Benchmarking range-dependent active sonar performance models: Scenarios and first results, In Akal, T., (Ed.), *Proceedings of the 10th European Conference on Underwater Acoustics*, Vol. 2, pp. 678–685. Conference held in Istanbul, Turkey, 5-9 July 2010.

Zampolli, M., Ainslie, M. A., and Schippers, P. (2010), Scenarios for benchmarking range-dependent active sonar performance models, *Proc. Institute of Acoustics*, 32, Pt. 2, 53–63.

This page intentionally left blank.

Annex A: Envelope of pulse and fathometer time series

We obtain the envelope of the coherent fathometer returns by a procedure which should be equivalent to a Hilbert transform. We define a $q_0(t)$ which corresponds to the $p_0(t)$ of Eq. (15) except that the `cos` is replaced by `sin`. For the source pulse this gives the mean squared pressure as

$$I_0(t) = \frac{|p_0(t)|^2 + |q_0(t)|^2}{2} = \frac{A_G}{2} \exp\left(-\frac{1}{2}(t\Delta\omega)^2\right). \tag{A.1}$$

For the fathometer time series, we calculate a $q(t)$ corresponding to the $p(t)$ of Eq. (11). The mean squared pressure $F(t)$ of the fathometers for Eq. (13) is then

$$F(t) = \frac{|p(t)|^2 + |q(t)|^2}{2} e^{-2\beta_w c_w t}. \tag{A.2}$$

From a computational point of view, with the carrier frequency ω_0 removed, the sampling rate for $F(t)$ can be decimated (we used a factor of 10, reducing to two points per cycle), and added to the incoherently-calculated reverberation time series.

This page intentionally left blank.

Distribution list

DRDC Atlantic TM 2011-323

Internal distribution

3 Library

2 Dale Ellis

1 Head/Underwater Sensing

1 Sean Pecknold

1 Paul Hines

1 Jim Theriault

Total internal copies: 9

External distribution

Department of National Defence

1 DRDKIM

Other Canadian Recipients

1 Library and Archives Canada
395 Wellington Street
Ottawa, ON K1A 0N4

International recipients

2 Applied Research Laboratory
The Pennsylvania State University
P. O. Box 30
State College, PA, 16804, USA
Attn: Dr. John R. Preston; Dr. Charles W. Holland

1 NATO Undersea Research Centre
Viale San Bartolomeo, 400
19126 La Spezia (SP), Italy
Attn: Dr. Chris Harrison, Dr. John Osler

1 TNO Stieltjesweg 1
2628 CK Delft
The Netherlands
Attn: Dr. Michael A. Ainslie

Total external copies: 6

Total copies: 15

DOCUMENT CONTROL DATA

(Security classification of title, body of abstract and indexing annotation must be entered when document is classified)

1. ORIGINATOR (The name and address of the organization preparing the document. Organizations for whom the document was prepared, e.g. Centre sponsoring a contractor's report, or tasking agency, are entered in section 8.)

Defence R&D Canada – Atlantic
PO Box 1012, Dartmouth NS B2Y 3Z7, Canada

2a. SECURITY CLASSIFICATION (Overall security classification of the document including special warning terms if applicable.)

UNCLASSIFIED

2b. CONTROLLED GOODS

(NON-CONTROLLED GOODS)
DMC A
REVIEW: GCEC JUNE 2010

3. TITLE (The complete document title as indicated on the title page. Its classification should be indicated by the appropriate abbreviation (S, C or U) in parentheses after the title.)

Calculations of reverberation and fathometer returns at short times using a straight-line ray-path model

4. AUTHORS (Last name, followed by initials – ranks, titles, etc. not to be used.)

Ellis, D. D.

5. DATE OF PUBLICATION (Month and year of publication of document.)	6a. NO. OF PAGES (Total containing information. Include Annexes, Appendices, etc.)	6b. NO. OF REFS (Total cited in document.)
February 2012	40	16

7. DESCRIPTIVE NOTES (The category of the document, e.g. technical report, technical note or memorandum. If appropriate, enter the type of report, e.g. interim, progress, summary, annual or final. Give the inclusive dates when a specific reporting period is covered.)

Technical Memorandum

8. SPONSORING ACTIVITY (The name of the department project office or laboratory sponsoring the research and development – include address.)

Defence R&D Canada – Atlantic
PO Box 1012, Dartmouth NS B2Y 3Z7, Canada

9a. PROJECT OR GRANT NO. (If appropriate, the applicable research and development project or grant number under which the document was written. Please specify whether project or grant.)	9b. CONTRACT NO. (If appropriate, the applicable number under which the document was written.)
11cb	

10a. ORIGINATOR'S DOCUMENT NUMBER (The official document number by which the document is identified by the originating activity. This number must be unique to this document.)	10b. OTHER DOCUMENT NO(s). (Any other numbers which may be assigned this document either by the originator or by the sponsor.)
DRDC Atlantic TM 2011-323	

11. DOCUMENT AVAILABILITY (Any limitations on further dissemination of the document, other than those imposed by security classification.)

(X) Unlimited distribution
( ) Defence departments and defence contractors; further distribution only as approved
( ) Defence departments and Canadian defence contractors; further distribution only as approved
( ) Government departments and agencies; further distribution only as approved
( ) Defence departments; further distribution only as approved
( ) Other (please specify):

12. DOCUMENT ANNOUNCEMENT (Any limitation to the bibliographic announcement of this document. This will normally correspond to the Document Availability (11). However, where further distribution (beyond the audience specified in (11)) is possible, a wider announcement audience may be selected.)

13. ABSTRACT (A brief and factual summary of the document. It may also appear elsewhere in the body of the document itself. It is highly desirable that the abstract of classified documents be unclassified. Each paragraph of the abstract shall begin with an indication of the security classification of the information in the paragraph (unless the document itself is unclassified) represented as (S), (C), or (U). It is not necessary to include here abstracts in both official languages unless the text is bilingual.)

A straight-line ray-path model has been developed to calculate reverberation and fathometer returns at short times. Previous calculations of reverberation at long ranges/times have shown good agreement among various models, with very little dependence on the receiver depth. However, at times less than a few seconds the steep-angle scattering and fathometer returns begin to dominate, so normal mode and other waveguide models begin to break down, but ray models are quite efficient. At very short times the fathometer returns completely dominate, and there is a strong dependence on the receiver depth. The reverberation is calculated assuming the scattered energy in the various multipath arrivals is summed incoherently. However, the fathometer returns are specular reflections and the pressure from each arrival should be summed coherently. The equations for the model are presented, and illustrated by a number of examples from Problem XI of the Reverberation Modeling Workshop. This problem has a vertically bistatic source-receiver geometry in 100 m of isovelocity water over a flat sand-like bottom with Lambert scattering. The pulse is a Gaussian-shaded CW, with a bandwidth of 1/20 of the centre frequency. In this model the calculations show that at higher frequencies (e.g., 3500 Hz) the individual fathometer returns can be clearly seen, but at lower frequencies (e.g., 250 Hz) the pulse is longer and the returns overlap. In this case the method of fathometer summation selected, coherent or incoherent, is significant as well as the details of the pulse shape. Particularly interesting is the receiver at the source depth (monostatic case) where a pair of fathometer returns have identical amplitudes and phases so add coherently, compared with a receiver just a half-wavelength apart, where the fathometers essentially cancel.

14. KEYWORDS, DESCRIPTORS or IDENTIFIERS (Technically meaningful terms or short phrases that characterize a document and could be helpful in cataloguing the document. They should be selected so that no security classification is required. Identifiers, such as equipment model designation, trade name, military project code name, geographic location may also be included. If possible keywords should be selected from a published thesaurus. e.g. Thesaurus of Engineering and Scientific Terms (TEST) and that thesaurus identified. If it is not possible to select indexing terms which are Unclassified, the classification of each should be indicated as with the title.)

reverberation modelling
benchmarks
Reverberation Modeling Workshop
Validation of Sonar Performance Tools
Pekeris model
Lambert's rule
fathometer returns
ray theory
Gaussian pulse

This page intentionally left blank.

Defence R&D Canada

Canada's leader in defence
and National Security
Science and Technology

R & D pour la défense Canada

Chef de file au Canada en matière
de science et de technologie pour
la défense et la sécurité nationale

DEFENCE DÉFENSE

www.drdc-rddc.gc.ca